galaxies

MDPI

Article

New Method to Detect and Characterize Active Be Star Candidates in Open Clusters

Anahí Granada [1,2,*], Maziar R. Ghoreyshi [3], Carol E. Jones [3] and Tõnis Eenmäe [4]

1 Centro Interdisciplinario de Telecomunicaciones, Electrónica, Computación y Ciencia Aplicada (CITECCA), Sede Andina, Universidad Nacional de Río Negro, Anasagasti 1463, San Carlos de Bariloche R8400AHN, Río Negro, Argentina
2 Consejo Nacional de Investigaciones Científicas y Técnicas (CONICET), Godoy Cruz 2290, Buenos Aires 1461, Argentina
3 Physics and Astronomy Department, The University of Western Ontario, London, ON N6A 3K7, Canada
4 Faculty of Science and Technology, University of Tartu, Observatooriumi 1, 61602 Tõravere, Estonia
* Correspondence: agranada@unrn.edu.ar

Abstract: With the aim of better understanding the physical conditions under which Be stars form and evolve, it is imperative to further investigate whether poorly studied young open clusters host Be stars. In this work, we explain how data from Gaia DR2 and DR3 can be combined to recover and characterize active Be stars in open clusters. We test our methodology in four open clusters broadly studied in the literature, known for hosting numerous Be stars. In addition, we show that the disk formation and dissipation approach that is typically used to model long term Be star variability, can explain the observed trends for Be stars in a (G_{DR3}-G_{DR2}) versus G_{DR3} plot. We propose that extending this methodology to other open clusters, and, in particular, those that are poorly studied, will help to increase the number of Be candidates. Eventually, Be stars may eclipse binary systems in open clusters.

Keywords: Be stars; early-type emission stars; circumstellar disks; early-type variable stars; open star clusters; Gaia

check for updates

Citation: Granada, A.; Ghoreyshi, M.R.; Jones, C.E.; Eenmäe, T. New Method to Detect and Characterize Active Be Star Candidates in Open Clusters. *Galaxies* **2023**, *11*, 37. https://doi.org/10.3390/galaxies11010037

Academic Editor: Jorick Sandor Vink

Received: 23 January 2023
Revised: 13 February 2023
Accepted: 16 February 2023
Published: 19 February 2023

1. Introduction

Be stars are rapidly rotating main sequence B-type stars that have exhibited hydrogen emission lines at least once, a signature of the presence of a circumstellar envelope, usually described in the viscous decretion disk framework [1]. Even though Be stars constitute about 30% of early B-type stars, or even more in some young open clusters [2–4], the mechanisms involved in the development of the disk are still under study, and neither the origin of the rapid rotation of these stars, nor how close to critical they rotate, is well understood [1]. In the single star scenario, stellar evolution allows stars with a sufficiently large initial angular momentum content to evolve towards the critical limit [5–7]. Episodes of mass transfer in binary systems [8,9] could also lead to the formation of a rapidly rotating star that could potentially become a Be star.

Following the single rotating star scenario, it is expected that clusters with log(age[Myr]) around 7.1 to 7.4 are likely host a number of Be stars, and, indeed, this is observed (e.g., [10]). In this framework, these authors proposed that the Be phenomenon is an evolutionary effect, appearing at the end of the main-sequence lifetime of a rapidly rotating B star.

Yet, why do some clusters of this age range host a very large fraction of Be stars while others have only a handful of them? Is this just an effect of small number statistics or are there *real* differences in the clusters where these stars form and evolve?

With the aim of better understanding the physical conditions under which Be stars form and evolve, it is imperative to further investigate whether poorly studied young open clusters host Be stars. This is not an easy task, because characterizing Be stars relies on obtaining spectroscopic data of individual stars, which is usually expensive in terms of telescope time. The results from spectroscopic surveys, such as the Apache Point Observatory Galactic Evolution Experiment (APOGEE) [11] or the Large sky Area Multi-Object fiber Spectroscopic Telescope (LAMOST) [12], have successfully increased the number of Be stars (e.g., Chojnowski et al. [13], Lin et al. [14], Vioque et al. [15], Wang et al. [16]). However, due to the transient nature of these objects, developing new methods of detecting Be candidates is called for. In particular, a new method, utilizing photometric archival data from Gaia Data Release 2 (DR2) [17] and Data Release 3 (DR3) [18], seems very promising, and devising such a method was the aim of the present article.

In Section 2, we explain how data from Gaia DR2 and DR3 can be combined to recover and characterize active Be stars in four broadly studied open clusters, two of which constitute the Double Cluster NGC869/NGC884. Then, in Section 3 we present a toy model of disc formation and dissipation around a B type star which can help explain the observations. Finally, we present our results and conclusions.

2. Materials and Methods

2.1. Gaia DR2 and DR3 Photometry

One of the main goals of the Gaia mission is to deliver multi-band photometry from the spectral energy distribution of stars in order to derive stellar fundamental parameters and identify peculiar objects [19]. Up to now, Gaia has provided three data releases (DRs). In particular, Gaia's second data release (DR2) was published during April, 2018, and Gaia Data Release 3 was split into the early release, called Gaia Early Data Release 3 (Gaia EDR3) and the full Gaia Data Release 3 (Gaia DR3),which was finally released in June, 2022. While DR2 spanned 22 months of data, (E)DR3 data spanned 34 months, including those of DR2.

At each Gaia release, a fundamental step in data processing, referred to as photometric external calibration, was performed. As a consequence, each release has its own definition of the set of passbands G, G_{BP} and G_{RP}. Basically, each of these three passbands changes between different releases. For this reason, a direct comparison of individual stars from different releases is usually discouraged [20]. Instead, for a comparison between releases it is recommended to use carefully selected datasets. For further details on Gaia photometry the reader is referred to Riello et al. [20], as well as the Gaia documentation pages.

In the present article, we proposed comparing Gaia DR2 and DR3 photometry for four well studied open clusters hosting numerous Be stars: the double cluster NGC869/NGC884, NGC663 and NGC7419.

2.2. Taking Advantage of the Variable Nature of Be Stars

First of all, it is important to recall that Be stars usually undergo photometric and spectroscopic variability on different timescales [1]. The characteristics of their mid- and long-term photometric variability, typically lasting from months to years, can be mostly explained in the Viscous Decretion Disk (VDD) framework [21] in terms of disk formation or dissipation processes, or due to disk perturbations (e.g., Rivinius et al. [1], Labadie-Bartz et al. [22], and references therein).

For the clusters under study, we claimed that stars which had not exhibited variability during the Gaia mission, small amplitude variable stars and, even, unresolved binaries, would not only have smaller error bars in Gaia photometric data than active Be stars, but would also define a narrow sequence in the (G_{DR3}-G_{DR2}) versus G_{DR3}. We refer to stars in this tight sequence as *stable stars*. Due to the typical amplitude of their long-term variability, of the order of one magnitude [23], active Be stars that exhibited variability during the Gaia mission would depart from this sequence. In this case, we describe stars with a significant disk variability within the epoch of each release as 'active'. Stars with a stable disk, or even those having variability much smaller than the duration of the mission, would also remain close to the narrow band of *stable stars*. In the next subsection we detail our findings for each cluster.

If the Gaia filters were identical between releases, the narrow band of *stable stars* would cluster around zero. As described above, this is not the case, as filters were redefined at each release [17,18]. In this work, we center our analysis on the Gaia G filter variability between DR2 and DR3, as in both releases the errors in the G band were significantly smaller than those of the other two bands, G_B and G_R [20].

2.3. Open Cluster Data

As mentioned previously, we focused on four galactic open clusters gathered in three different samples, with ages between 14 and 40 Myr, notorious for their large number of Be stars, which have been broadly studied in the literature: the double cluster NGC869/NGC884 [24–26], NGC663 [3,27,28] and NGC7419 [2]. As these are rich in Be stars, it was expected that a fraction of them would either be forming or dissipating a disk in the epoch of observation.

For each cluster, we considered as cluster members those stars having membership probabilities larger than 0.5, according to [29]. All the data analyzed in this work are provided in the Appendix A.

3. Results

3.1. NGC869/NGC884

The pair consisting of NGC869 and NGC884, centered at right ascension, RA, and declination, dec, 34.741°, +57.134° and 35.584°, +57.149°, respectively, is a physically bound system. The distance to NGC869 is 2246 pc, its age is 12.9 Myr and its mean absorption in the V band is 1.749, while for NGC 884 the distance is 2150 pc, with an age of 15.4 Myr and a mean extinction in the V band of 1.709, according to [30], and, in agreement with [29,31,32], within the errors.

For this double cluster, we selected objects with $G_{DR3} < 14.5$ because all their known B stars are more than one magnitude brighter than this value. To start with, we investigated errors in the G band for these bright cluster members. In Figure 1a we plotted the errors in G_{DR3} ($errG_{DR3}$) versus G_{DR3}. Small violet symbols indicate cluster members, and red squares indicate known Be stars from the literature [25,33]. Cyan symbols indicate stars classified as eclipsing binaries (EBs) in SIMBAD, and green triangles are non-Be pulsating variable stars in NGC 884 by [34]. Blue pentagons belong to the RS Canum Venaticorum class, a type of active eclipsing binary star, according to [35].

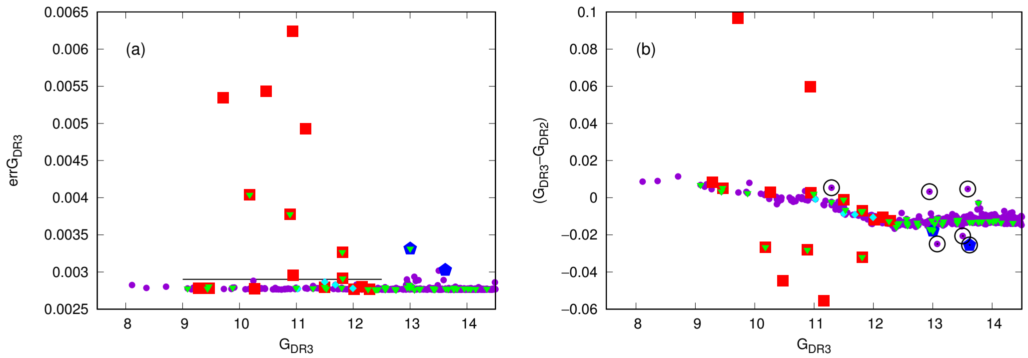

Figure 1. Data for NGC869/NGC884. (**a**) Error in the G_{DR3} band versus G_{DR3} magnitude. (**b**) (G_{DR3}-G_{DR2}) versus G_{DR3}. Violet small symbols indicate cluster members, and red squares indicate known Be stars, cyan symbols indicate stars classified as eclipsing binaries, green triangles are pulsating variable stars. Blue penthagons belong to the RS Canum Venaticorum class. The open black circles enclose objects that depart significantly from the tight relation for stable stars.

The values of $errG_{DR3}$ centered around a median value of 0.00277 for most stars in the range of G plotted. Performing a detailed analysis of these photometric errors would be a complex task [20] and was beyond the scope of the present article. However, and very interestingly, all stars with $G_{DR3} < 12.5$ with $errG_{DR3} > 0.0029$ are known Be stars. Values of $G_{DR3} > 12.5$ delimited the transition from late B to early A stars at around G = 14 mag, and, also, intriguingly, two of the stars with the largest departure from the median value were stars classified as rotational variables by [35], and one of them had shown pulsations [34] .

In Figure 1b we plotted (G_{DR3}-G_{DR2}) versus G_{DR3}. Again, and not surprisingly, we can clearly see that the seven Be stars with the largest $errG_{DR3}$ also departed from the violet trend, which indicated that these objects were changing significantly between the two different releases. In addition, we can see that while two of the Be stars faded (above the violet trend), another five Be stars brightened (below the violet trend). In Section 4, we interpret the behavior of these objects in the context of a disk formation/dissipation scheme, as seen from different inclination angles.

An inspection of Figure 1b led us to propose that six stars departed from the violet trend that gathered most stars, or *stable stars*. These are indicated with open black circles and were considered to be Be candidates. Interestingly, one of them was an EB. Together with the 16 known Be stars and other interesting variable stars, we listed the Be candidates, as shown in Table A1.

3.2. NGC663

The open cluster NGC663 is located at RA of 26.586° and dec of +61.212°, at a distance of 2950 pc, having an age of 30 Myr and an average extinction in the V band of 2.18 [32].

Similar to the double cluster, we considered objects with $G_{DR3} < 14.5$, which easily included B-type stars.

The color coding in Figure 2 is identical to Figure 1: violet symbols indicate cluster members in the quoted range, while red squares are known Be stars. Figure 2a shows that stars with $errG_{DR3} > 0.0029$ and $G_{DR3} < 13.5$ were all known Be stars. There were two stars beyond this limit, with $errG_{DR3} > 0.0029$, that were not known Be stars. Figure 2b shows that most of the Be stars were at, or above, the violet trend of *stable* stars. Only three Be stars were below. An eye inspection of Figure 2 led us to propose 5 Be candidates, which are indicated as open circles, in addition to the 30 known Be stars. We list them in Table A2.

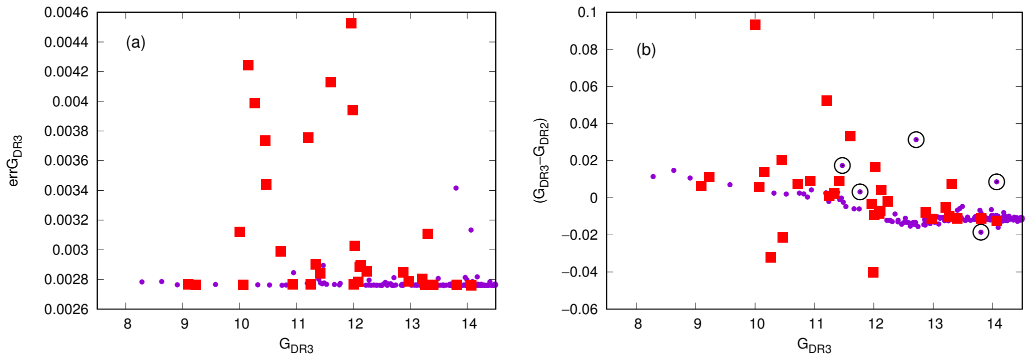

Figure 2. Data for the cluster NGC 663. (**a**) Error in the G_{DR3} band versus G_{DR3} magnitude. (**b**) (G_{DR3}-G_{DR2}) versus G_{DR3}. Violet small symbols indicate cluster members and red squares indicate known Be stars. The open black circles enclose objects that depart significantly from the tight relation for stable stars.

3.3. NGC7419

The cluster NGC 7419 is located at RA 343.579°, dec +60.814°, and, according to the literature, at a distance between 3105 pc [30] and 3236 pc [36]. Different values for its age are found in the literature, between 5 Myr [30] and 30 Myr [31]. The number of red supergiant and Be stars observed in this cluster may favor an intermediate age of 14 Myr [37]. The average extinction in the V band of this cluster is large, with a value of 4.291 [30].

NGC 7419 is more distant than the other three clusters mentioned above, and suffers frpm a heavy intra-cluster reddening, as can be deduced from its broad Color-Magnitude Diagram [2]. Objects close to a magnitude of G = 17 have been classified as Be stars by these authors, so this is why we included all objects brighter than G_{EDR3} = 18 in this analysis.

Figure 3a shows that all but one star with $G_{DR3} < 15$ and $errG_{DR3} > 0.003$ were known Be stars. As in the previous cases, Be stars were characterized by their large errors when compared to the non-Be cluster stars (*stable stars*). In Figure 3b, the values of G_{DR3}-G_{DR2} had a significantly larger dispersion than those in Figures 1b and 2b. This is why we color-coded according to the (B_G-R_G) color of each star. Red open squares indicate Be stars and the empty red square corresponds to a Be star for which no B_G or R_G was available. Black open circles in Figure 3b enclose stars that significantly departed from the main *stable star* distribution. The dispersion was much larger in this highly reddened cluster, so we arbitrarily considered stars with G_{DR3}-$G_{DR2} > -0.015$ or G_{DR3}-$G_{DR2} < -0.034$ as candidates. Using this criteria, we obtained 19 new Be candidates, two of which were actually EBs, in addition to the 37 known Be stars that were cluster members with probability higher than 0.5, according to [29]. We list the Be candidates and EBs in Table A3.

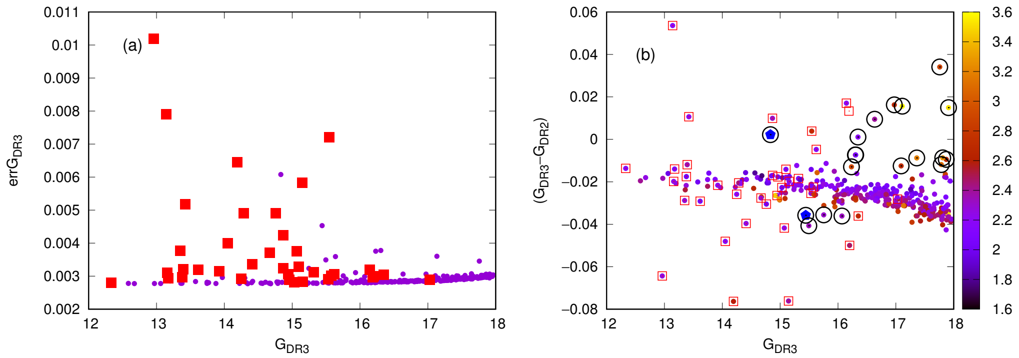

Figure 3. (**a**) The same as Figure 1a for the cluster NGC 7419. (**b**) The same plot as Figure 1b, but the color coding corresponds to the color ($B_G - R_G$). The blue symbols indicate EBs.

3.4. A Model for Be Disk Formation and Dissipation

It was beyond the scope of the present article to model each Be star developing, or not developing, variability between the DR2 and DR3 releases, in detail. However, we could gain insight as to whether a typical model for disk formation and dissipation could explain the observed trends for Be stars in the (G_{DR3}-G_{DR2}) versus GDR3 plot.

With this aim, we used the SINGLEBE code [38,39] in order to compute the dynamical 1D surface density of an isothermal viscous decretion disk. SINGLEBE is a hydrodynamic code, which solves the time-dependent fluid equations [40] in the thin disk approximation. The vertical hydrostatic equilibrium solution, with a power-law scale height $H = H_0(r/R)^{1.5}$, and H_0 being the scale height at the base of the disk, r being the distance from the central star and R the stellar radius, was used to convert the output of SINGLEBE to a volume density. Then, this density structure was used by the 3D non-LTE Monte Carlo radiative transfer code HDUST [41,42], which calculated the synthetic observables from the star plus disk system, including the spectral energy distribution, SED.

In the models presented here, we considered only two different stellar models, corresponding to B2 and B7 stars. Their stellar parameters were identical to those presented by Ghoreyshi et al. [43] and the stars were considered to rotate at 75% of their critical speeds. We assumed that the disks were built up for 50 years with a steady mass injection rate of 7.7 $\times$ 10^{-9} M$\odot$/year and 1.14 $\times$ 10^{-10} M$\odot$/year for the B2 and B7 stellar model, respectively, which were typical mass loss rates for these spectral types [43]. After build-up, the disks were allowed to dissipate for 50 years.

For the B2 star, a base surface density of 0.8 g cm^{-2} (volume density, $\rho_0 = 2.13 \times 10^{-11}$ g cm^{-3}) was adopted. Similarly, for the B7 star a disk base surface density of 0.1 g cm^{-2} (volume density, $\rho_0 = 4.4 \times 10^{-12}$ g cm^{-3}) was used. We considered the inclination angles of 0° (pole-on), 30°, 70° and 90° (equator-on), as seen by an observer.

Along the synthetic build-up/dissipation sequence, for each SED, we computed Gaia magnitudes G, G_B and G_R using the passbands and zero point magnitudes available in the Gaia DR2[1] and DR3[2] web pages, which enabled us to make lightcurves. Of course, this type of synthetic lightcurve represents average long term variability of Be stars, and does not capture other short term variability often observed in Be stars.

We note that, for most stars, Gaia DR3 provides time-averaged magnitudes in the different bands, and only for some stars is a time-series also available [20].

It was the goal of this article to interpret these average values delivered by Gaia DR2 and DR3. To do so, at each time of the build-up/dissipation sequence, we computed the simple average values of the G, G_B and G_R within the previous 22 months for DR2 and 34 months for DR3, and assumed that, prior to the disk development, there was no disk at all.

Then, at each time of the build-up/dissipation sequence, we computed the difference between the average G magnitude DR3 (G_{DR3}) and the average G magnitude DR2 (G_{DR2}), *twelve months before*. This was to account for the fact that DR3 included 12 more months of data than DR2 data.

We denoted $(G_{DR3}\text{-}G_{DR2})_0$ as the value of $(G_{DR3}\text{-}G_{DR2})$ for the diskless star. In Figure 4a we plotted the predicted $(G_{DR3}\text{-}G_{DR2})$, normalized relative to $(G_{DR3}\text{-}G_{DR2})_0$, versus G_{DR3} for the B2 stellar model with different colors indicating different inclination angles. The dotted part of the curve corresponds to buildup, while the continuous line indicates the dissipation phase. Full circles mark the start of the cycle. Coloured squares show the average value within a full disk formation–dissipation cycle (100 years in the case presented here), but a similar result would be obtained for a shorter cycle, when formation and dissipation have the same length. This suggested that stars that undergo full cycles within the Gaia releases might tend to cluster above the zero level.

Figure 4b is the same Figure 4a for the B7 model. While the global behavior was similar for both stellar models, a larger departure from the zero level was obtained for the earlier spectral type.

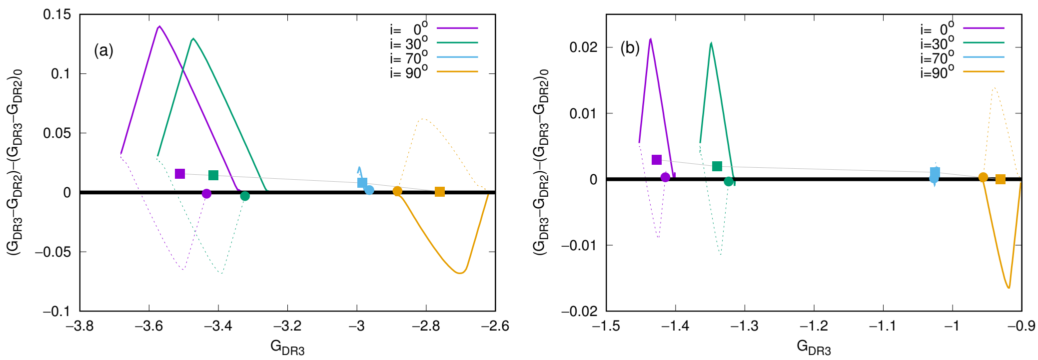

Figure 4. (**a**) Modeled $(G_{DR3}\text{-}G_{DR2})$, normalized relative to the value at time zero, with subindex 0, versus G_{DR3} for the B2 model. Different colors indicate different inclination angles. The dotted part of the curve corresponds to build-up and the continuous line to dissipation. The black line indicates the zero level (no variability). The full circles indicate the beginning of the cycle. The squares indicate the average value within a complete cycle and the gray line joins these squares. (**b**) Same as (**a**) for the B7 model.

We can see that for small inclination angles the values of $(G_{DR3}\text{-}G_{DR2})\text{-}(G_{DR3}\text{-}G_{DR2})_0$ were positive during the disc build-up phase and negative during dissipation, while for large inclinations the opposite was observed. Moreover, the predicted differences in brightness were in good agreement with what was observed for early and late Be stars, as seen in the previous subsections.

Interestingly, if the dissipation phases were longer than the formation phases, as suggested in the literature [44,45], then observation of stars during their disk dissipation stage would be more likely. Furthermore, observation of active Be stars with a small inclination angle, with positive values of G_{DR3}-G_{DR2}, and those with large inclination angles with negative values, relative to the stable stars would be more likely.

We investigated this point for the Double Cluster NGC869/NGC884, for which we had extensive data for cluster B-type stars. Figure 5 is similar to Figure 1b, but normalized to the stable star sequence, through a linear piecewise fit. This way, we could directly compare the data with the models of Figure 4. The color coding indicates the projected rotational velocity (in km s^{-1}) for the stars with available data. In Table A1 we indicate the reference for each velocity measurement.

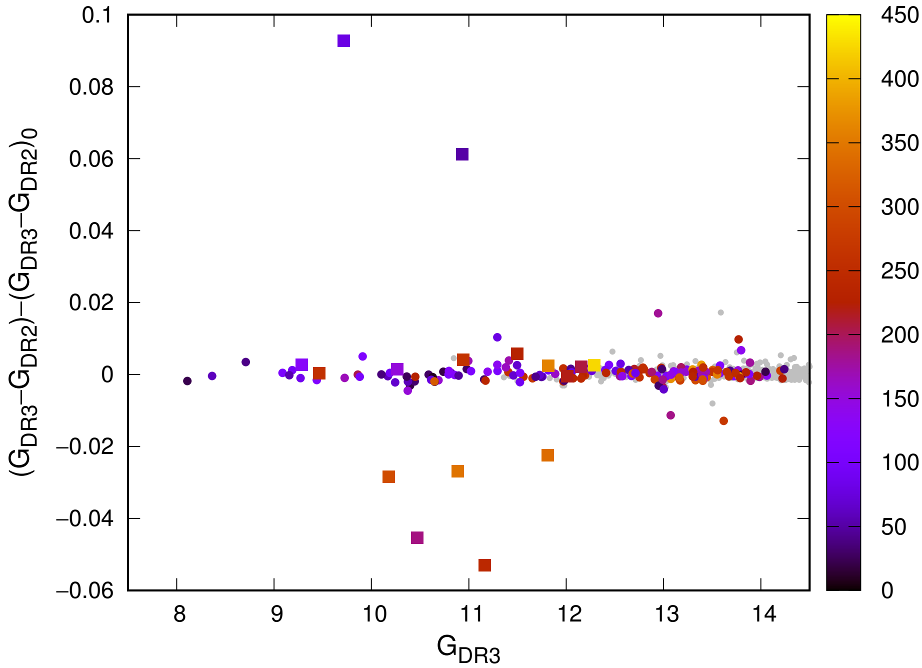

Figure 5. Similar to Figure 1b, but normalized to the *stable star* sequence, color coded according their projected rotational velocity (in units of km s^{-1}).

We can see that the stars with a positive difference in G magnitude between the two releases had small projected rotational velocities, while among the five stars with negative differences, three had values larger than 300 km s^{-1} and only one had a projected rotational velocity smaller than 200 km s^{-1}.

4. Discussion

We showed that the error in the Gaia G band and G_{DR3}-G_{DR2} were both excellent quantities to detect active Be stars in open clusters. Additionally, the latter quantity could be useful for insight into the inclination angle of the star as well. This could be particularly useful for stars for which no Gaia spectroscopic data, nor lightcurve, is yet available.

Increasing the number of Be candidates in poorly studied open clusters certainly helps in better understanding the environments where these stars form and evolve, so this paper opens a new opportunity in the Be star research community.

Among the few objects without a Be classification, that departed from the tight stellar sequence in the G_{DR3}-G_{DR2} versus G_{DR3} diagram, we found one RS Canum Venaticorum star in the Double Cluster and two Eclipsing Binary stars in NGC 7419. These types of binaries with short period variability, could exhibit large differences within different releases, which could certainly influence the average magnitude of the object if a different proportion of light minima were caught between DR2 and DR3.

Among the new Be candidates, we could potentially have a few eclipsing binaries, which are themselves interesting objects to study in clusters (e.g., [46] and references therein). The study of these objects allows us to accurately measure stellar parameters of the binary stars, having the same age and chemical composition, and, together with the cluster isochrone studies, put solid constraints on stellar evolution models.

Author Contributions: Conceptualization, A.G.; Formal analysis, A.G. and M.R.G.; Investigation, A.G., M.R.G., C.E.J. and T.E.; Methodology, A.G., M.R.G. and C.E.J.; Project administration, A.G.; Resources, A.G.; Writing—original draft, A.G., M.R.G., C.E.J. and T.E. All authors have read and agreed to the published version of the manuscript.

Funding: A.G. acknowledges the research project from Universidad Nacional de Río Negro PI-UNRN2020 40-B-890. M.R.G. acknowledges the grant awarded by the Western University Postdoctoral Fellowship Program (WPFP). C.E.J. wishes to acknowledge support through the Natural Sciences and Engineering Research Council of Canada. T.E. gratefully acknowledges financial support from the Estonian Ministry of Education and Research through the Estonian Research Council institutional research funding IUT40-1, from the European Union European Regional Development Fund project KOMEET 2014-2020.4.01.16-0029 and from Marie Skłodowska-Curie Research and Innovation Staff Exchanges RISE grant "Physics of Extreme Massive Stars", agreement no 823734. The authors thank the APC Discount Voucher from Western University b7f7871016d98506.

Institutional Review Board Statement: Not applicable.

Informed Consent Statement: Not applicable.

Data Availability Statement: This work made use of data from the European Space Agency (ESA) mission *Gaia* https://www.cosmos.esa.int/gaia (accessed on 15 February 2023), processed by the *Gaia* Data Processing and Analysis Consortium , DPAC, https://www.cosmos.esa.int/web/gaia/dpac/consortium (accessed on 15 February 2023). Funding for the DPAC was provided by national institutions; in particular, the institutions participating in the *Gaia* Multilateral Agreement. This research made use of the SIMBAD database, operated at CDS, Strasbourg, France.

Acknowledgments: The authors thank the reviewers of this manuscript for their constructive feedback.

Conflicts of Interest: The authors declare no conflict of interest.

Appendix A

Appendix A.1. NGC869/NGC884

We present Table A1 that contains relevant data for the Double Cluster. The first columns indicate position (RA and Dec), then Gaia DR2 brightness in G,GB and GR passbands, Gaia DR3 brightness in G, its error , GB and GR passbands. The column "Group" indicates different types of interesting objects: **1** corresponds to known Be stars either from SIMBAD or [47], **2** Eclipsing binaries from SIMBAD, **3** β Ceph starsfrom SIMBAD, **4** Pulsational variable according to [34], **5** Candidate Be stars according to the present work and **6** RS Canum Venaticorum stars according to [35]. The asterisk in the last column indicates the two-peak separation of an intense near IR hydrogen line from APOGEE [48], for a Be star without V sin(i) available in the literature.

Table A1. Relevant data for variable stars of the Double Cluster. See text for a description.

RA	DEC	G_{DR2}	GB_{DR2}	GR_{DR2}	G_{DR3}	$errG_{DR3}$	GB_{DR3}	GR_{DR3}	Group	$V\sin(i)$	Ref.
34.9493	57.1110	10.8742	11.1487	10.3406	10.9341	0.0062	11.2242	10.4313	1	51	[24]
34.5823	57.1462	12.1688	12.3107	11.8610	12.1583	0.0028	12.3166	11.8579	1	207	[24]
34.8701	57.1179	10.9403	11.2315	10.4876	10.9430	0.0030	11.2193	10.4826	1	264	[24]
34.7368	57.1286	12.0243	12.2062	11.6728	12.0125	0.0028	12.2074	11.6691	1	219	[24]
34.7263	57.1582	10.2641	10.4417	9.9624	10.2670	0.0028	10.4313	9.9551	1	151	[24]
34.8644	57.1382	9.2773	9.4955	8.9362	9.2856	0.0028	9.4795	8.9269	1	127	[24]
34.7244	57.1395	9.4608	9.6454	9.1537	9.4659	0.0028	9.6308	9.1476	1	258	[24]
35.8538	57.3176	10.5171	10.9499	9.9197	10.4723	0.0054	10.8947	9.8582	1	187	[33]
35.4289	57.0918	11.2214	11.4029	10.9038	11.1660	0.0049	11.3458	10.7962	1	242	[24]
35.7402	57.3940	12.3000	12.5393	11.8834	12.2877	0.0028	12.5352	11.8769	1	426	*
35.4706	57.1664	9.6194	9.9104	9.1552	9.7160	0.0053	9.9660	9.2597	1	79	[24]
35.7503	57.2039	11.8232	12.0240	11.4525	11.8161	0.0029	12.0239	11.4485	1–4	360	[24]
35.7095	57.1474	11.8411	12.0159	11.5078	11.8091	0.0033	12.0022	11.4536	1–4	338	[24]
35.7674	57.1274	10.2063	10.4515	9.8175	10.1797	0.0040	10.4128	9.7811	1–4	300	[49]
35.4353	57.1812	11.4977	11.7296	11.1105	11.4967	0.0028	11.7209	11.1072	1–4	229	[33]
35.5103	57.1557	10.9163	11.1057	10.5768	10.8882	0.0038	11.0594	10.5437	1–4	345	[26]
35.5127	57.1348	11.5075	11.6759	11.1950	11.4989	0.0029	11.6788	11.1861	2		
35.7670	57.1691	12.0040	12.2191	11.6201	11.9934	0.0028	12.2141	11.6150	2		
35.5034	57.1255	11.0243	11.1382	10.8016	11.0235	0.0028	11.1329	10.7970	2	108	[24]
35.5651	57.2247	11.6959	11.8949	11.3398	11.6868	0.0028	11.8861	11.3327	2	42	[24]
34.7403	57.1383	10.9792	11.1288	10.6958	10.9792	0.0028	11.1266	10.6901	3	29	[24]
35.5116	57.1403	9.8773	10.0418	9.6027	9.8797	0.0028	10.0249	9.5944	3–4	101	[24]
35.4569	57.0266	13.0194	13.2094	12.6567	13.0016	0.0033	13.2051	12.6650	6–4	67	[24]
35.4656	57.2516	13.0872	13.3849	12.6004	13.0761	0.0028	13.3813	12.5933	4		
35.5632	57.1613	12.2744	12.4501	11.9271	12.2618	0.0028	12.4466	11.9218	4	74	[24]
35.3907	57.0655	12.9961	13.2280	12.5881	12.9839	0.0028	13.2265	12.5862	4	33	[24]
35.3685	57.1429	12.7480	12.9406	12.3892	12.7346	0.0028	12.9385	12.3857	4		
35.6083	57.1148	13.6839	13.8988	13.2909	13.6709	0.0028	13.8914	13.2902	4	261	[24]
35.5357	57.1245	9.0813	9.2409	8.8145	9.0882	0.0028	9.2231	8.8073	4	106	[24]
35.6736	57.1745	13.7828	14.0480	13.3374	13.7699	0.0028	14.0369	13.3322	4		
35.7984	57.1721	9.4555	9.6140	9.1837	9.4608	0.0028	9.5966	9.1803	4		
35.6791	57.2053	14.0299	14.2640	13.5991	14.0169	0.0028	14.2585	13.5901	4		
35.5610	57.1038	12.7677	12.9296	12.4428	12.7528	0.0028	12.9300	12.4399	4	261	[24]
35.5740	57.1038	13.9658	14.1573	13.6065	13.9531	0.0028	14.1542	13.6056	4		
35.3572	57.0727	13.4464	13.6912	13.0258	13.4346	0.0028	13.6834	13.0205	4	170	[24]
35.6499	57.2089	14.3629	14.6035	13.9438	14.3493	0.0028	14.5967	13.9436	4		
35.3535	57.0403	13.1761	13.3697	12.8174	13.1619	0.0028	13.3636	12.8114	4	318.4	[50]
35.5546	57.0228	13.0086	13.2169	12.6250	12.9914	0.0028	13.2075	12.6215	4	203	[24]
35.8416	57.0071	13.6374	13.8506	13.2549	13.6243	0.0028	13.8428	13.2505	4		
35.7392	57.0089	12.4026	12.5392	12.1126	12.3868	0.0028	12.5385	12.1088	4		
35.5774	57.1972	11.5349	11.7150	11.1979	11.5283	0.0028	11.7130	11.1917	4	112	[24]
35.8269	57.2589	13.4186	13.6603	13.0026	13.4065	0.0028	13.6522	12.9944	4		
35.4569	57.1393	11.2951	11.4272	11.0250	11.2929	0.0028	11.4336	11.0207	4	136	[33]
35.4455	57.1649	13.4276	13.6494	13.0349	13.4139	0.0028	13.6431	13.0301	4	116	[24]
35.4415	57.0836	12.5769	12.7887	12.1972	12.5632	0.0028	12.7839	12.1909	4	248	[24]
35.4350	57.1483	11.8044	11.9496	11.5095	11.7970	0.0028	11.9506	11.5091	4	67	[26]
35.5934	57.1841	13.7854	14.0243	13.3578	13.7725	0.0028	14.0223	13.3545	4	371	[24]
35.5205	57.1005	13.1930	13.3577	12.8670	13.1802	0.0028	13.3576	12.8634	4	154	[24]
35.5464	57.1067	14.1656	14.3810	13.7706	14.1522	0.0028	14.3773	13.7698	4		
35.6210	57.0288	12.9666	13.1444	12.6263	12.9498	0.0028	13.1403	12.6211	4	30	[24]
35.5146	57.1190	12.5907	12.7674	12.2621	12.5758	0.0028	12.7574	12.2585	4	141	[24]
35.5571	57.0881	13.0428	13.1915	12.7294	13.0287	0.0028	13.1966	12.7270	4	108	[24]
35.5302	57.2033	12.5708	12.7529	12.2199	12.5593	0.0028	12.7542	12.2175	4	81	[24]
35.5116	57.1479	12.4469	12.6046	12.1357	12.4332	0.0028	12.6024	12.1317	4		
35.5968	57.1682	14.0780	14.3092	13.6478	14.0658	0.0028	14.3022	13.6473	4		
35.4447	57.1241	10.9932	11.1498	10.7138	10.9954	0.0028	11.1461	10.7073	4	169	[24]
35.6619	57.1955	12.4247	12.6093	12.0751	12.4104	0.0028	12.6058	12.0690	4	241	[24]
35.5470	57.1093	13.8381	14.0395	13.4629	13.8253	0.0028	14.0377	13.4634	4		

Table A1. *Cont.*

RA	DEC	G_{DR2}	GB_{DR2}	GR_{DR2}	G_{DR3}	$errG_{DR3}$	GB_{DR3}	GR_{DR3}	Group	$V\sin(i)$	Ref.
35.6244	57.2080	9.4355	9.6155	9.1426	9.4389	0.0028	9.5958	9.1318	4	116	[24]
34.4696	57.1242	12.9408	13.1021	12.6158	12.9441	0.0029	13.1196	12.6285	5	180	[50]
34.8142	57.0939	13.0988	13.3639	12.6514	13.0739	0.0029	13.3422	12.6408	5	185	[24]
34.8834	57.1218	13.6437	13.9132	13.1905	13.6183	0.0030	13.9044	13.1716	5–6	272	[24]
35.4618	57.2643	13.5838			13.5885	0.0029			5		
35.5035	57.1597	11.2881	11.4393	11.0116	11.2935	0.0028	11.4408	11.0079	5	79	[24]
35.7434	57.0802	13.7731	14.0176	13.3364	13.7703	0.0028	14.0095	13.3302	5–4	228	[24]

EBs are identified with the symbol * next to the RA value.

Appendix A.2. NGC663

Be candidates of NGC663 proposed in this article as described in Section 3.2. All the data for the star cluster members [29] are available online in Gaia DR2 and DR3.

Table A2. Be candidates of NGC663. See text for a description.

RA	DEC	G_{DR2}	GB_{DR2}	GR_{DR2}	G_{DR3}	$errG_{DR3}$	GB_{DR3}	GR_{DR3}
26.1345	61.0357	11.7643	11.9475	11.4064	11.7675	0.0025	11.9430	11.3990
26.5405	61.2060	12.6804	12.9845	12.1887	12.7118	0.0028	13.0160	12.2311
26.5817	61.2636	11.4527	11.8009	10.9543	11.4701	0.0029	11.7979	10.9528
26.6511	61.2011	14.0593	14.4175	13.5280	14.0679	0.0031	14.4219	13.5397
26.8232	61.3506	13.8222	14.1819	13.2778	13.8036	0.0034	14.1629	13.2602

Appendix A.3. NGC7419

17 Be candidates of NGC7419 proposed in this article as described in Section 3.3, and 2 EBs. All the data for the star cluster members [29] are available online in Gaia DR2 and DR3.

Table A3. Be candidates of NGC7419. See text for a description.

RA	DEC	G_{DR2}	GB_{DR2}	GR_{DR2}	G_{DR3}	$errG_{DR3}$	GB_{DR3}	GR_{DR3}
343.3217	60.8266	16.2447	17.9178	14.9481	16.2317	0.0038	17.8946	14.9813
343.3976	60.7236	17.8185	19.6804	16.4386	17.8098	0.0030	19.7270	16.4657
343.5181	60.7933	17.1032	18.5614	15.8439	17.0907	0.0029	18.5888	15.8691
343.5192	60.7611	16.3070	17.4165	15.0216	16.2996	0.0029	17.4446	15.0234
343.5481	60.8442	15.7882	16.9885	14.6624	15.7526	0.0030	16.9658	14.6565
343.5646	60.8256	16.6244	17.6384	15.2435	16.6339	0.0031	17.6608	15.2752
343.5754	60.8065	16.3449			16.3460	0.0030	17.3938	15.1945
343.5891 *	60.8316	15.4774	16.6915	14.3236	15.4416	0.0045	16.6786	14.3248
343.5972	60.8085	16.9569	17.8607	15.2027	16.9731	0.0031	17.9529	15.2617
343.6272	60.7987	17.7249	18.8056	15.8962	17.7590	0.0035	18.8473	15.9640
343.6694	60.7861	15.5368	16.7586	14.4025	15.4961	0.0035	16.7250	14.3865
343.6737	60.8330	17.3693	19.2339	16.0482	17.3605	0.0030	19.2504	16.0646
343.6776	60.7436	17.7969	19.5841	16.4758	17.7850	0.0030	19.5888	16.4931
343.6802	60.8398	17.0955			17.1111	0.0030	19.3139	15.7285
343.6902	60.8920	16.3127	17.3359	15.2738	16.3054	0.0028	17.3156	15.2716
343.7105	60.7716	16.1045	17.3278	14.9738	16.0684	0.0030	17.2937	14.9631
343.7106	60.8031	17.8798	19.3287	16.6495	17.8704	0.0030	19.3064	16.6636
343.7752 *	60.7680	14.8305	15.8472	13.7992	14.8327	0.0061	15.8423	13.8122
343.8161	60.8345	17.8965			17.9114	0.0031	20.0666	16.5431

EBs are identified with the symbol * next to the RA value.

Notes

[1] https://www.cosmos.esa.int/web/gaia/iow_20180316 (accessed on 15 February 2023).

[2] https://www.cosmos.esa.int/web/gaia/edr3-passbands (accessed on 15 February 2023).

References

1. Rivinius, T.; Carciofi, A.C.; Martayan, C. Classical Be stars. Rapidly rotating B stars with viscous Keplerian decretion disks. *Astron. Astrophys. Rev.* **2013**, *21*, 69. [CrossRef]
2. Pigulski, A.; Kopacki, G. NGC 7419: An open cluster rich in Be stars. *Astron. Astrophys. Suppl. Ser.* **2000**, *146*, 465–469. [CrossRef]
3. Pigulski, A.; Kopacki, G.; Kołaczkowski, Z. The young open cluster NGC 663 and its Be stars. *Astron. Astrophys.* **2001**, *376*, 144–153. [CrossRef]
4. Mathew, B.; Subramaniam, A.; Bhatt, B.C. Be phenomenon in open clusters: Results from a survey of emission-line stars in young open clusters. *Mon. Not. R. Astron. Soc.* **2008**, *388*, 1879–1888. [CrossRef]
5. Ekström, S.; Meynet, G.; Maeder, A.; Barblan, F. Evolution towards the critical limit and the origin of Be stars. *Astron. Astrophys.* **2008**, *478*, 467–485. [CrossRef]
6. Georgy, C.; Ekström, S.; Granada, A.; Meynet, G.; Mowlavi, N.; Eggenberger, P.; Maeder, A. Populations of rotating stars. I. Models from 1.7 to 15 $M_\odot$ at Z = 0.014, 0.006, and 0.002 with Ω/Ω_{crit} between 0 and 1. *Astron. Astrophys.* **2013**, *553*, A24. [CrossRef]
7. Granada, A.; Ekström, S.; Georgy, C.; Krtička, J.; Owocki, S.; Meynet, G.; Maeder, A. Populations of rotating stars. II. Rapid rotators and their link to Be-type stars. *Astron. Astrophys.* **2013**, *553*, A25. [CrossRef]
8. Bodensteiner, J.; Shenar, T.; Sana, H. Investigating the lack of main-sequence companions to massive Be stars. *Astron. Astrophys.* **2020**, *641*, A42. [CrossRef]
9. El-Badry, K.; Conroy, C.; Quataert, E.; Rix, H.W.; Labadie-Bartz, J.; Jayasinghe, T.; Thompson, T.; Cargile, P.; Stassun, K.G.; Ilyin, I. Birth of a Be star: An APOGEE search for Be stars forming through binary mass transfer. *Mon. Not. R. Astron. Soc.* **2022**, *516*, 3602–3630. [CrossRef]
10. Fabregat, J.; Torrejón, J.M. On the evolutionary status of Be stars. *Astron. Astrophys.* **2000**, *357*, 451–459.
11. Majewski, S.R. APOGEE—SDSS-III's Other Milky Way Experiment. In *Proceedings of the American Astronomical Society Meeting Abstracts #219*; 2012; Volume 219, p. 205.06.
12. Luo, A.L.; Zhao, Y.H.; Zhao, G.; Deng, L.C.; Liu, X.W.; Jing, Y.P.; Wang, G.; Zhang, H.T.; Shi, J.R.; Cui, X.Q.; et al. The first data release (DR1) of the LAMOST regular survey. *Res. Astron. Astrophys.* **2015**, *15*, 1095. [CrossRef]
13. Chojnowski, S.D.; Whelan, D.G.; Wisniewski, J.P.; Majewski, S.R.; Hall, M.; Shetrone, M.; Beaton, R.; Burton, A.; Damke, G.; Eikenberry, S.; et al. High-Resolution H-Band Spectroscopy of Be Stars With SDSS-III/Apogee: I. New Be Stars, Line Identifications, and Line Profiles. *Astron. J.* **2015**, *149*, 7. [CrossRef]
14. Lin, C.C.; Hou, J.L.; Chen, L.; Shao, Z.Y.; Zhong, J.; Yu, P.C. Searching for classical Be stars in LAMOST DR1. *Res. Astron. Astrophys.* **2015**, *15*, 1325. [CrossRef]
15. Vioque, M.; Oudmaijer, R.D.; Schreiner, M.; Mendigutía, I.; Baines, D.; Mowlavi, N.; Pérez-Martínez, R. Catalogue of new Herbig Ae/Be and classical Be stars. A machine learning approach to Gaia DR2. *Astron. Astrophys.* **2020**, *638*, A21. [CrossRef]
16. Wang, L.; Li, J.; Wu, Y.; Gies, D.R.; Liu, J.Z.; Liu, C.; Guo, Y.; Chen, X.; Han, Z. Identification of New Classical Be Stars from the LAMOST Medium Resolution Survey. *Astrophys. J. Suppl. Ser.* **2022**, *260*, 35. [CrossRef]
17. Gaia Collaboration; Brown, A.G.A.; Vallenari, A.; Prusti, T.; de Bruijne, J.H.J.; Babusiaux, C.; Bailer-Jones, C.A.L.; Biermann, M.; Evans, D.W.; Eyer, L.; et al. Gaia Data Release 2. Summary of the contents and survey properties. *Astron. Astrophys.* **2018**, *616*, A1. [CrossRef]
18. Gaia Collaboration; Vallenari, A.; Brown, A.G.A.; Prusti, T.; de Bruijne, J.H.J.; Arenou, F.; Babusiaux, C.; Biermann, M.; Creevey, O.L.; Ducourant, C.; et al. Gaia Data Release 3: Summary of the content and survey properties. *arXiv* **2022**, arXiv:2208.00211.
19. Gaia Collaboration; Prusti, T.; de Bruijne, J.H.J.; Brown, A.G.A.; Vallenari, A.; Babusiaux, C.; Bailer-Jones, C.A.L.; Bastian, U.; Biermann, M.; Evans, D.W.; et al. The Gaia mission. *Astron. Astrophys.* **2016**, *595*, A1. [CrossRef]
20. Riello, M.; De Angeli, F.; Evans, D.W.; Montegriffo, P.; Carrasco, J.M.; Busso, G.; Palaversa, L.; Burgess, P.W.; Diener, C.; Davidson, M.; et al. Gaia Early Data Release 3. Photometric content and validation. *Astron. Astrophys.* **2021**, *649*, A3. [CrossRef]
21. Lee, U.; Osaki, Y.; Saio, H. Viscous excretion discs around Be stars. *Mon. Not. R. Astron. Soc.* **1991**, *250*, 432–437. [CrossRef]
22. Labadie-Bartz, J.; Pepper, J.; McSwain, M.V.; Bjorkman, J.E.; Bjorkman, K.S.; Lund, M.B.; Rodriguez, J.E.; Stassun, K.G.; Stevens, D.J.; James, D.J.; et al. Photometric Variability of the Be Star Population. *Astron. J.* **2017**, *153*, 252. [CrossRef]
23. Haubois, X.; Mota, B.C.; Carciofi, A.C.; Draper, Z.H.; Wisniewski, J.P.; Bednarski, D.; Rivinius, T. Dynamical Evolution of Viscous Disks around Be Stars. II. Polarimetry. *Astrophys. J.* **2014**, *785*, 12. [CrossRef]
24. Strom, S.E.; Wolff, S.C.; Dror, D.H.A. B Star Rotational Velocities in h and χ Persei: A Probe of Initial Conditions during the Star Formation Epoch? *Astron. J.* **2005**, *129*, 809–828. [CrossRef]
25. McSwain, M.V.; Gies, D.R. The Evolutionary Status of Be Stars: Results from a Photometric Study of Southern Open Clusters. *Astrophys. J. Suppl. Ser.* **2005**, *161*, 118. [CrossRef]
26. Huang, W.; Gies, D.R.; McSwain, M.V. A Stellar Rotation Census of B Stars: From ZAMS to TAMS. *Astrophys. J.* **2010**, *722*, 605. [CrossRef]
27. Pandey, A.K.; Upadhyay, K.; Ogura, K.; Sagar, R.; Mohan, V.; Mito, H.; Bhatt, H.C.; Bhatt, B.C. Stellar contents of two young open clusters: NGC 663 and 654. *Mon. Not. R. Astron. Soc.* **2005**, *358*, 1290–1308. [CrossRef]
28. Torrejon, J.M.; Fabregat, J.; Bernabeu, G.; Alba, S. Be stars in open clusters. II. Balmer line spectroscopy. *Astron. Astrophys. Suppl. Ser.* **1997**, *124*, 329–347. [CrossRef]

29. Cantat-Gaudin, T.; Jordi, C.; Vallenari, A.; Bragaglia, A.; Balaguer-Núñez, L.; Soubiran, C.; Bossini, D.; Moitinho, A.; Castro-Ginard, A.; Krone-Martins, A.; et al. A Gaia DR2 view of the open cluster population in the Milky Way. *Astron. Astrophys.* **2018**, *618*, A93. [CrossRef]
30. Dias, W.S.; Monteiro, H.; Moitinho, A.; Lépine, J.R.D.; Carraro, G.; Paunzen, E.; Alessi, B.; Villela, L. Updated parameters of 1743 open clusters based on Gaia DR2. *Mon. Not. R. Astron. Soc.* **2021**, *504*, 356–371. [CrossRef]
31. Kharchenko, N.V.; Piskunov, A.E.; Roeser, S.; Schilbach, E.; Scholz, R.D. VizieR Online Data Catalog: Milky Way global survey of star clusters. II. (Kharchenko+, 2013). *Vizier Online Data Cat.* **2013**, *355*, 80053.
32. Cantat-Gaudin, T.; Anders, F.; Castro-Ginard, A.; Jordi, C.; Romero-Gómez, M.; Soubiran, C.; Casamiquela, L.; Tarricq, Y.; Moitinho, A.; Vallenari, A.; et al. Painting a portrait of the Galactic disc with its stellar clusters. *Astron. Astrophys.* **2020**, *640*, A1. [CrossRef]
33. Huang, W.; Gies, D.R. Stellar Rotation in Young Clusters. I. Evolution of Projected Rotational Velocity Distributions. *Astrophys. J.* **2006**, *648*, 580–590. [CrossRef]
34. Saesen, S.; Briquet, M.; Aerts, C.; Miglio, A.; Carrier, F. Pulsating B-type Stars in the Open Cluster NGC 884: Frequencies, Mode Identification, and Asteroseismology. *Astron. J.* **2013**, *146*, 102. [CrossRef]
35. Chen, X.; Wang, S.; Deng, L.; de Grijs, R.; Yang, M.; Tian, H. The Zwicky Transient Facility Catalog of Periodic Variable Stars. *Astrophys. J. Suppl. Ser.* **2020**, *249*, 18. [CrossRef]
36. Cantat-Gaudin, T.; Anders, F. Clusters and mirages: Cataloguing stellar aggregates in the Milky Way. *Astron. Astrophys.* **2020**, *633*, A99. [CrossRef]
37. Marco, A.; Negueruela, I. NGC 7419 as a template for red supergiant clusters. *Astron. Astrophys.* **2013**, *552*, A92. [CrossRef]
38. Okazaki, A.T.; Bate, M.R.; Ogilvie, G.I.; Pringle, J.E. Viscous effects on the interaction between the coplanar decretion disc and the neutron star in Be/X-ray binaries. *Mon. Not. R. Astron. Soc.* **2002**, *337*, 967–980. [CrossRef]
39. Okazaki, A.T. Theory vs. Observation of Circumstellar Disks and Their Formation. In *Proceedings of the Active OB-Stars: Laboratories for Stellar and Circumstellar Physics*; Okazaki, A.T., Owocki, S.P., Stefl, S., Eds.; Astronomical Society of the Pacific Conference Series, ASP: San Francisco, CA, USA, 2007; Volume 361, p. 230.
40. Lynden-Bell, D.; Pringle, J.E. The evolution of viscous discs and the origin of the nebular variables. *Mon. Not. R. Astron. Soc.* **1974**, *168*, 603–637. [CrossRef]
41. Carciofi, A.C.; Bjorkman, J.E. Non-LTE Monte Carlo Radiative Transfer. I. The Thermal Properties of Keplerian Disks around Classical Be Stars. *Astrophys. J.* **2006**, *639*, 1081–1094. [CrossRef]
42. Carciofi, A.C.; Bjorkman, J.E. Non-LTE Monte Carlo Radiative Transfer. II. Nonisothermal Solutions for Viscous Keplerian Disks. *Astrophys. J.* **2008**, *684*, 1374–1383. [CrossRef]
43. Ghoreyshi, M.R.; Jones, C.E.; Granada, A. Angular momentum loss rates in Be stars determined by the viscous decretion disc model. *Mon. Not. R. Astron. Soc.* **2023**, *518*, 30–38. [CrossRef]
44. Vieira, R.G.; Carciofi, A.C.; Bjorkman, J.E.; Rivinius, T.; Baade, D.; Rímulo, L.R. The life cycles of Be viscous decretion discs: Time-dependent modelling of infrared continuum observations. *Mon. Not. R. Astron. Soc.* **2017**, *464*, 3071–3089. [CrossRef]
45. Rímulo, L.R.; Carciofi, A.C.; Vieira, R.G.; Rivinius, T.; Faes, D.M.; Figueiredo, A.L.; Bjorkman, J.E.; Georgy, C.; Ghoreyshi, M.R.; Soszyński, I. The life cycles of Be viscous decretion discs: Fundamental disc parameters of 54 SMC Be stars. *Mon. Not. R. Astron. Soc.* **2018**, *476*, 3555–3579. [CrossRef]
46. Southworth, J.; Clausen, J.V. Eclipsing Binaries in Open Clusters. *Astrophys. Space Sci.* **2006**, *304*, 199–202. [CrossRef]
47. Laur, J.; Kolka, I.; Eenmäe, T.; Tuvikene, T.; Leedjärv, L. Variability survey of brightest stars in selected OB associations. *Astron. Astrophys.* **2017**, *598*, A108. [CrossRef]
48. Jönsson, H.; Holtzman, J.A.; Allende Prieto, C.; Cunha, K.; García-Hernández, D.A.; Hasselquist, S.; Masseron, T.; Osorio, Y.; Shetrone, M.; Smith, V.; et al. APOGEE Data and Spectral Analysis from SDSS Data Release 16: Seven Years of Observations Including First Results from APOGEE-South. *Astron. J.* **2020**, *160*, 120. [CrossRef]
49. Glebocki, R.; Gnacinski, P. VizieR Online Data Catalog: Catalog of Stellar Rotational Velocities (Glebocki+ 2005). *Vizier Online Data Cat.* **2005**, *III*, 244.
50. Sun, W.; Duan, X.W.; Deng, L.; de Grijs, R.; Zhang, B.; Liu, C. Exploring the Stellar Rotation of Early-type Stars in the LAMOST Medium-resolution Survey. I. Catalog. *Astrophys. J. Suppl. Ser.* **2021**, *257*, 22. [CrossRef]